

# Numerical Analysis of Large-Scale Finite Periodic Arrays Using a Macro Block-Characteristic Basis Function Method

Keisuke Konno, *Member, IEEE*, Qiang Chen, *Senior Member, IEEE*, and Robert J. Burkholder, *Fellow, IEEE*

**Abstract**—Numerical analysis of a large-scale finite periodic array is accurate but quite costly when the array is analyzed as a finite array. The computational cost for the numerical analysis can be reduced greatly when the array is approximated as an infinite periodic structure. However, the edge effect that strongly affects the active impedance or current distribution of the array elements near the edge is neglected. In this paper, a macro block-characteristic basis function method (MB-CBFM) for numerical analysis of a large-scale finite periodic array with a uniform amplitude and linear phased excitation is proposed. The MB-CBFM utilizes blocks and macro blocks to group the elements in order to reduce its computational cost without degrading accuracy. Numerical simulations demonstrate that the CPU time and computer memory of the MB-CBFM are  $O(N)$  when the size of array is sufficiently large.

**Index Terms**—Arrays, characteristic basis function method (CBFM), fast solvers, method of moments (MoM), microstrip arrays, periodic structures.

## I. INTRODUCTION

A LARGE-SCALE finite periodic array is widely used as a phased array antenna [1], [2], frequency selective surface [3], and reflectarray [4]–[7]. The design and performance of such an array is obtained using a numerical simulation technique such as the method of moments (MoM) [8]. Although powerful computers are available now, numerical analysis of the large-scale finite periodic array using the MoM is still costly because its CPU time and computer memory are  $O(N^3)$  and  $O(N^2)$ , respectively, where  $N$  is the total number of unknowns.

Extensive efforts have been made to reduce the computational cost of the MoM for periodic structures. The periodic MoM (PMM) is one of the most powerful techniques [9], [10].

Manuscript received July 12, 2016; revised April 26, 2017; accepted July 31, 2017. Date of publication August 7, 2017; date of current version October 5, 2017. This work was supported in part by JSPS KAKENHI under Grant 25420394 and Grant 26820137 and in part by the JSPS Postdoctoral Fellowships for Research Abroad. (*Corresponding author: Keisuke Konno.*)

K. Konno is with the Department of Electrical and Communications Engineering, Tohoku University, Sendai 980-8579, Japan, and also with the Department of Electrical and Computer Engineering, ElectroScience Laboratory, The Ohio State University, Columbus, OH 43210 USA (e-mail: konno@ecei.tohoku.ac.jp).

Q. Chen is with the Department of Electrical and Communications Engineering, Tohoku University, Sendai 980-8579, Japan.

R. J. Burkholder is with the Department of Electrical and Computer Engineering, ElectroScience Laboratory, The Ohio State University, Columbus, OH 43210 USA.

Color versions of one or more of the figures in this paper are available online at <http://ieeexplore.ieee.org>.

Digital Object Identifier 10.1109/TAP.2017.2736526

The large-scale periodic array is approximated as an infinite array and a unit cell analysis is performed when the PMM is applied. The PMM is quite computationally efficient but completely neglects the finite truncation edge effect which leads to severe inaccuracies for elements near edges.

Various fast MoM iterative algorithms have also been developed for numerical analysis of large-scale finite periodic arrays. The multilevel fast multipole algorithm (MLFMA) [11], [12], adaptive integral method (AIM) [13], or the conjugate gradient-fast Fourier transform (CG-FFT) greatly reduce computational cost of the MoM [14]–[16]. Both CPU time per iteration and computer memory of the MLFMA and CG-FFT are  $O(N \log N)$ . However, these fast MoMs are based on iterative matrix solvers and are plagued by ill-conditioned problems.

Another approach is to reduce the order of the problem size using macro basis functions (MBFs) so that a direct solver may be applied. It has been demonstrated that MBF methods are helpful in order to deal with microstrip array antennas or filters efficiently [17]–[19]. Synthetic functions expansion approach is a kind of MBF method and its performance has been demonstrated via numerical analysis of general 3-D structures [20]. The subdomain (SED) basis function method [21], [22] and the characteristic basis function method (CBFM) [23] are types of MBF methods and can reduce the number of unknowns. Both the SED basis function method and the CBFM have been applied for numerical analysis of the large-scale finite array [24]–[27]. However, the MBF method is only used to solve an element or subarray problem in these papers. As a result, authors finally resort to iterative solvers, such as the fast multipole method, FFT, or AIM, in order to deal with the large-scale entire array problem because the number of unknowns is still proportional to that of the elements or subarrays. To the best of our knowledge, an MBF method which utilizes array theory to reduce the number of unknowns has not been developed.

In this paper, a novel CBFM for numerical analysis of the large-scale finite periodic array is proposed. The proposed CBFM, which is named a macro block-CBFM (MB-CBFM), mainly builds on the conventional CBFM shown in [23], and this paper expands the work in [28] and [29]. The MB-CBFM uses blocks and macro blocks to drastically reduce the number of unknowns to be solved. A block contains a single cell of the periodic structure, and a macro block is made up of a number of blocks and depends on the array geometry.

Eigenvector decomposition is applied to the block current and the characteristic basis functions (CBFs) for the block are obtained without by direct solution. According to array theory, the CBFs for the macro blocks are obtained efficiently from those of the blocks without extra computational cost. The resultant reduced matrix can be solved using direct solvers even when the number of the array elements is quite large because the size of the reduced matrix is independent of the number of array elements. Moreover, the MB-CBFM can deal with an ill-conditioned problem efficiently because it is iteration free. Numerical examples are shown and the performance of the MB-CBFM is verified quantitatively.

## II. MACRO BLOCK-CHARACTERISTIC BASIS FUNCTION METHOD

In general, a linear system obtained using the MoM is

$$\mathbf{Z}\mathbf{I} = \mathbf{V} \quad (1)$$

where  $\mathbf{Z}$  is an  $N \times N$  impedance matrix,  $\mathbf{I}$  is an unknown  $N \times 1$  current vector, and  $\mathbf{V}$  is a known  $N \times 1$  voltage vector. Equation (1) can be divided into block matrix equations when a periodic array of identical elements is assumed

$$\begin{bmatrix} \mathbf{Z}_{11}^b & & \cdots & & \mathbf{Z}_{1M}^b \\ & \ddots & & & \\ \vdots & & \mathbf{Z}_{ii}^b & 0 & \vdots \\ & \mathbf{Z}_{ij}^b & & \ddots & \\ \mathbf{Z}_{M1}^b & \cdots & & & \mathbf{Z}_{MM}^b \end{bmatrix} \begin{bmatrix} \mathbf{I}_1^b \\ \vdots \\ \mathbf{I}_i^b \\ \vdots \\ \mathbf{I}_M^b \end{bmatrix} = \begin{bmatrix} \mathbf{V}_1^b \\ \vdots \\ \mathbf{V}_i^b \\ \vdots \\ \mathbf{V}_M^b \end{bmatrix} \quad (2)$$

where  $\mathbf{Z}_{ij}^b$  is a  $K \times K$  block impedance matrix between the  $i$ th array element and  $j$ th array element,  $\mathbf{I}_i^b$  is a  $K \times 1$  unknown block current vector of the  $i$ th array element, and  $\mathbf{V}_i^b$  is a  $K \times 1$  known voltage vector of the  $i$ th array element. Here,  $M$  is the total number of array elements and  $K$  is the number of unknowns in one element, i.e.,  $N = MK$ . The block defined here is called a block. According to a theory of MBFs, the unknown block current vector is expanded using MBFs, here, CBFs

$$\mathbf{I}_i^b = \sum_{k=1}^K \alpha_{(i,k)} \mathbf{J}_{(i,k)}^b \quad \text{for } i = 1, 2, \dots, M \quad (3)$$

where  $\alpha_{(i,k)}$  is an unknown weight coefficient of  $\mathbf{J}_{(i,k)}^b$ , which is the  $k$ th CBF of the  $i$ th element. The CBF  $\mathbf{J}_{(i,k)}^b$  must be computed in advance, first by solving the following extended matrix equation:

$$\mathbf{J}_i^e = (\mathbf{Z}_{ii}^e)^{-1} \mathbf{V}_i^e \quad \text{for } i = 1, 2, \dots, M \quad (4)$$

where  $\mathbf{J}_i^e$  is a  $(2L+1)^2 K \times 1$  current vector of the  $i$ th extended block,  $\mathbf{Z}_{ii}^e$  is the  $(2L+1)^2 K \times (2L+1)^2 K$   $i$ th extended block self-impedance matrix, and  $\mathbf{V}_i^e$  is the  $(2L+1)^2 K \times 1$   $i$ th extended block voltage vector. The extended block is introduced here in order to include the mutual coupling effect of the surrounding elements into the block current.  $L$  is the width of the edge regions and also indicates the edge region of a macro block as explained later. For example, a central

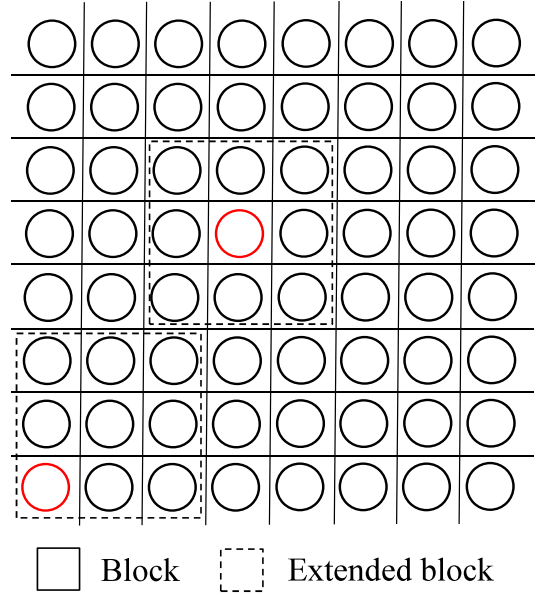


Fig. 1. Block division of an  $8 \times 8$  loop array for computing CBFs in blocks ( $L = 1$ ).

element in an extended block is surrounded by eight elements for  $L = 1$  and 24 elements for  $L = 2$ . An example of the block and extended block is shown in Fig. 1 for  $L = 1$ . It has been verified that this approach works well in order to include the mutual coupling effect of the surrounding structure into the block current [21], [23]. A part of  $\mathbf{J}_i^e$  corresponding to the  $i$ th block is kept as a block current  $\mathbf{J}_i^b$  and the other part is discarded. Finally, the CBFs  $\mathbf{J}_{(i,k)}^b$  are obtained as a result of eigenvector decomposition of  $\mathbf{J}_i^b$

$$\mathbf{J}_{(i,k)}^b = (\mathbf{J}_i^b \cdot \mathbf{e}_{(i,k)}) \mathbf{e}_{(i,k)} \quad \text{for } k = 1, 2, \dots, K \quad (5)$$

where  $\mathbf{e}_{(i,k)}$  is the  $k$ th eigenvector of the  $i$ th block self-impedance matrix,  $\mathbf{Z}_{ii}^b$ , and  $\mathbf{J}_i^b \cdot \mathbf{e}_{(i,k)}$  is the dot product.  $\mathbf{J}_{(i,k)}^b$  is a set of  $K$  orthogonal eigenvectors because  $\mathbf{Z}_{ii}^b$  is symmetric when the Galerkin method is used to obtain  $\mathbf{Z}$ . The set of  $K$  orthogonal eigenvectors is complete as a basis function for the block including  $K$  unknowns. Therefore, the MB-CBFM requires no secondary basis functions as are obtained in the conventional CBFM [23].

In order to obtain the unknown weight coefficient  $\alpha_{(i,k)}$  efficiently, the macro blocks shown in Fig. 2 are defined. Here, it is assumed that the array has a uniform amplitude and linear phase excitation. Under this assumption, it can be said that the current distribution of blocks inside the same macro block is uniform except for phase difference. Therefore, it is found that each CBF of the blocks has the same weight coefficient in (3) as all the other blocks in the same macro block.

According to this assumption, the number of weight coefficients to be obtained is reduced greatly.

The CBFs of the same blocks are joined with each other and the CBF of the  $p$ th macro block is obtained

$$\begin{aligned} \mathbf{J}_{(p,k)}^{mb} &= (\mathbf{J}_{(1,k)}^b, \mathbf{J}_{(2,k)}^b, \dots, \mathbf{J}_{(M'(p),k)}^b) \quad \text{for } k = 1, 2, \dots, K \\ \mathbf{J}_{(1,k)}^b &= \dots = \mathbf{J}_{(M'(p),k)}^b \end{aligned} \quad (6)$$

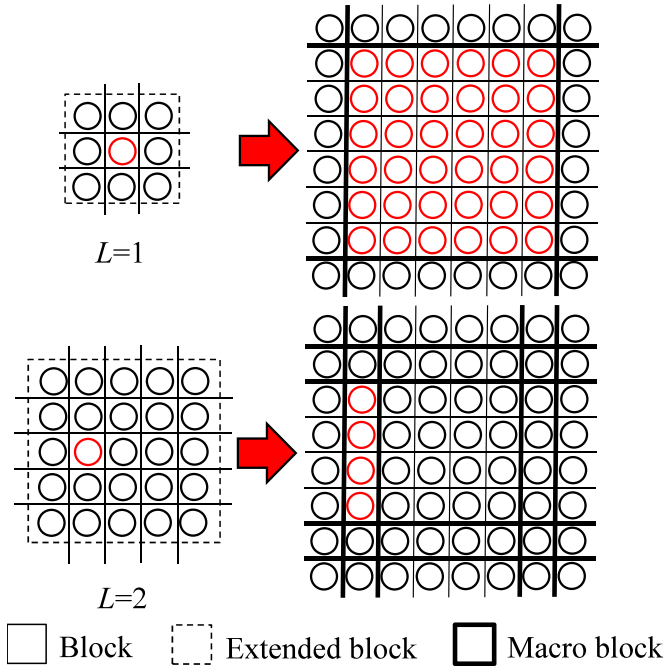


Fig. 2. Block division of an  $8 \times 8$  loop array for computing CBFs in macro blocks and reduced matrix ( $L = 1$  and  $2$ ).  $L$  is the width of the edge regions. In this case, the edge regions are one and two element wide. Red elements indicate correspondence of CBFs between blocks and macro blocks as an example.

where  $\mathbf{J}_{(p,k)}^{mb}$  is the  $k$ th joined CBF of the  $p$ th macro block and  $M'(p)$  is the number of blocks in the  $p$ th macro block. Using (6), (3) is transformed into

$$\mathbf{I}_p^b = \sum_{k=1}^K \alpha_{(p,k)} \mathbf{J}_{(p,k)}^{mb} \quad \text{for } p = 1, 2, \dots, P \quad (7)$$

where  $P$  is the total number of macro blocks and  $P = (2L + 1)^2$ . The macro blocks at the edges of the array only include blocks in a single row or column, but the CBFs in the macro block are obtained in the same manner. After that, the MoM system of equations is given in terms of the vector  $\mathbf{u}$  as

$$\sum_{i=1}^P \sum_{k=1}^K \alpha_{(p,k)} \mathbf{u}_{(p,k)} = \mathbf{V} \quad (\mathbf{u}_{(p,k)} = [[\mathbf{Z}_{1p}^{mb} \mathbf{J}_{(p,k)}^{mb}] [\mathbf{Z}_{2p}^{mb} \mathbf{J}_{(p,k)}^{mb}] \cdots [\mathbf{Z}_{Pp}^{mb} \mathbf{J}_{(p,k)}^{mb}]]^T). \quad (8)$$

A  $PK \times PK$  reduced matrix is obtained after the Galerkin method is applied to (8). The unknown weight coefficients are obtained from the reduced matrix.

As shown in (3), the total number of unknowns is  $N = MK$  when the conventional CBFM with the block division is applied. Of course, the optimum block division derived in [30] or singular value decomposition is helpful in order to reduce the number of unknowns when the problem is solved using the conventional CBFM. However, the computational cost for the computation of CBFs, and for computation of the reduced matrix equation are the tradeoff. As a result, it is difficult to reduce the computational cost greatly when the conventional CBFM is applied. On the other hand, the MB-CBFM uses eigenvector decomposition of the block current in order

TABLE I  
ORDER OF CPU TIME OF THE MB-CBFM

Calculation of impedance matrix	$O(N)$
Calculation of CBFs in blocks	$O(P^3 N^3 / M^3) \approx O(P^3 K^3)$ where $M$ is $O(N)$
Calculation of $\mathbf{u}$ vectors	$O(PK^2 N)$
Calculation of reduced matrix	$O(PK^2 N)$
Inversion of reduced matrix	$O(P^3 N^3 / M^3) \approx O(P^3 K^3)$ where $M$ is $O(N)$

to obtain CBFs. A complete set of CBFs for the blocks can be obtained efficiently without resorting an iterative process to find primary and secondary basis functions of the conventional CBFM [23]. In addition, macro block CBFs are obtained efficiently from those of the blocks without extra computational cost. As a result, the number of unknowns is greatly reduced from  $N$  to  $PK = (2L + 1)^2 K$  when the MB-CBFM is applied. The size of the reduced matrix ( $= PK \times PK$ ) is independent of the number of array elements and is much smaller than that of the original  $N \times N$  matrix. Therefore, the reduced matrix can always be solved easily using direct solvers such as Gaussian elimination even when the number of array elements is large. The computational cost to solve is  $O(P^3 K^3)$  but is negligibly small because  $K \ll N$  for large-scale periodic arrays. Therefore, the total computational cost of the MB-CBFM is expected to be reduced greatly.

The order of CPU time of the MB-CBFM is shown in Table I. The MB-CBFM is for a large-scale periodic array and it can be assumed that the number of elements  $M$  is proportional to the number of unknowns  $N$ , i.e.,  $M = O(N)$ . Moreover, it is assumed that the periodicity is fully utilized. Under these assumptions, the order of the CPU time of the MB-CBFM is  $O(N)$ , the time taken to fill the impedance matrix. It is noted from Table I that the edge region of the array impacts the CPU time of the MB-CBFM because the CPU time is approximately proportional to  $PK^2 N = (2L + 1)^2 K^2 N$  for a rectangular array.

It is expected that the edge region of the array could have more or less impact on the total CPU time for nonrectangular arrays, depending on the number of nonsimilar edges. It is interesting that the CPU time is impacted less as the shape of the array antenna approaches to circular because the circular array has no corners. The order of computer memory of the MB-CBFM is omitted here but is also  $O(N)$ .

### III. NUMERICAL SIMULATION

In order to verify the performance of the MB-CBFM, two numerical examples shown in Figs. 3 and 4 are analyzed. The dimensions of a helical array on an infinite ground plane are set to  $D = 0.2$  m,  $p = 0.1$  m,  $a = 0.003$  m,  $s = 0.05$  m,  $h = 0.25$  m, and  $d_x = d_y = 0.75$  m. The dimensions and constitutive parameters of a microstrip dipole array embedded in a double-layered medium backed by an infinite ground plane are set to  $l = 0.005$  m,  $2\Delta x = 0.001$  m,  $t_1 = 0.002$  m,  $t_2 = 0.001$  m,  $d_x = d_y = 0.007$  m,  $\epsilon_r^1 = 2.6$ ,  $\epsilon_r^2 = 2.15$ , and  $\mu_r^1 = \mu_r^2 = 1$ . The operating frequencies are  $f = 0.3$  and 20 GHz for the helical array and the dipole array, respectively.

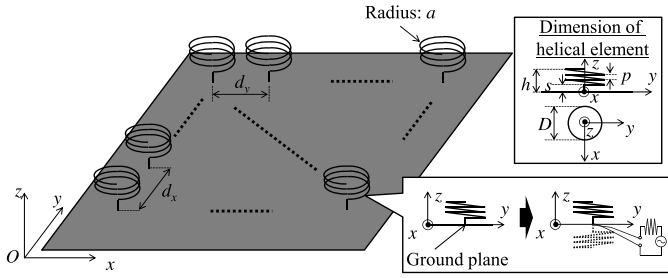


Fig. 3. Helical array antenna on an infinite ground plane.

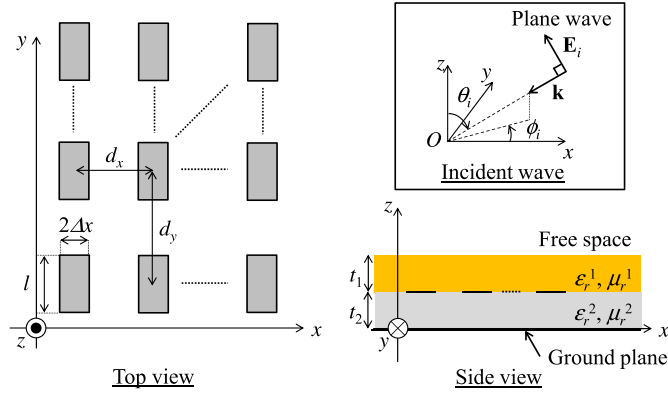


Fig. 4. Microstrip dipole array antenna embedded in double-layered medium.

Richmond's MoM is used for numerical analysis of the helical array antenna on an infinite ground plane with piecewise sinusoidal wire basis functions [31]. The MoM with the layered media Green's function is used for numerical analysis of the microstrip array [32], [33]. Piecewise sinusoidal functions are used as basis/testing functions for the printed metallic elements. The fourfold integrals over the spatial coordinates are evaluated as a sum of double integrals via a coordinate transformation [34]. An interpolation method using a recursive Taylor expansion is used in order to calculate the layered media impedance matrix efficiently [35]. The effect of a ground plane is included in the numerical simulation using image theory. The number of segments in a single array element including its image is  $K = 49$  and 14 for the helical array and the dipole array, respectively. All numerical simulations in this paper were implemented on an Intel Core2 Duo E8400 3 GHz processor with 4 GB RAM. Periodicity is fully utilized in our code. The reduced matrix equation obtained from a uniform and in-phase excitation is solved for a plane wave scattering problem and a radiation problem. A linear phase array factor multiplies the CBFs in order to obtain the current distribution for an oblique incidence scattering problem or beam scanning problem approximately without having to refill the impedance matrix or resolve for the CBFs.

The active impedance of a  $15 \times 15$  helical array antenna is shown in Fig. 5. It is found that the active impedance of each element obtained using the MB-CBFM agrees well with that of the full-wave matrix solution. In particular, the accuracy of the active impedance of an element in the edge region

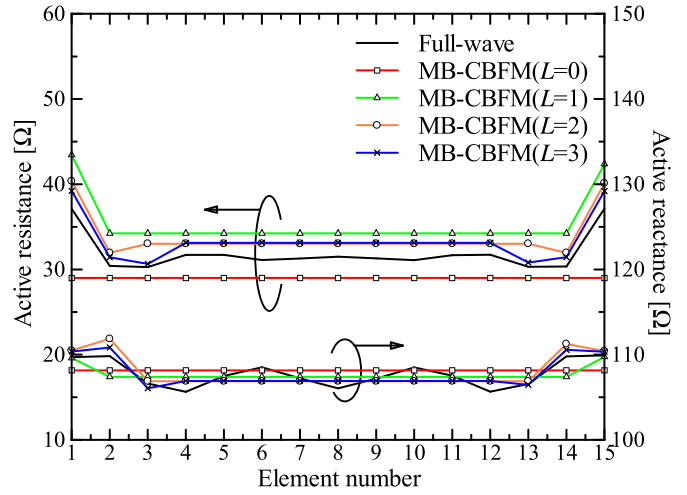
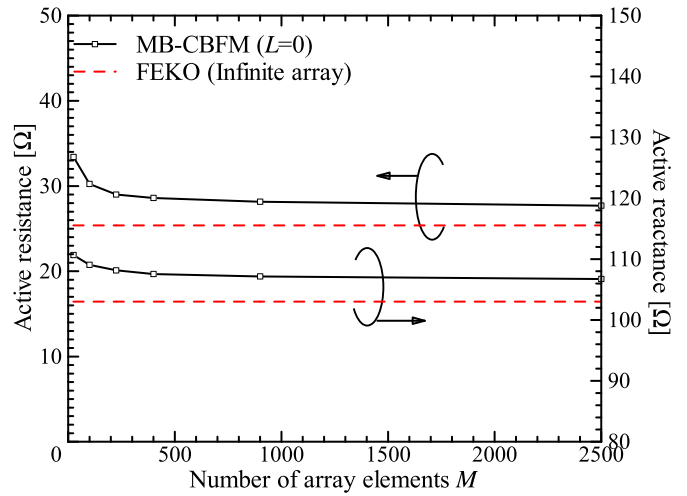

 Fig. 5. Active impedance of a  $15 \times 15$  helical antenna array. The outermost row along the  $y$ -axis with in-phase and uniform excitation is plotted.


Fig. 6. Convergence of active impedance of a helical array antenna (in-phase and uniform excitation).

of the array obtained using the MB-CBFM is enhanced as  $L$  increases.

On the other hand, the active impedance of elements in the central region of the array obtained using the MB-CBFM is uniform because of our initial assumption. Convergence of the active impedance of elements obtained using the MB-CBFM with respect to the size of the array is shown in Fig. 6. In order to simplify the discussion, results obtained using the MB-CBFM with  $L = 0$  are only compared with those of an infinite array obtained using FEKO. The MB-CBFM with  $L = 0$  neglects the edge effect and assumes that the current distribution of all elements in the array is uniform. As a result, the active impedance of all elements in the array obtained using the MB-CBFM with  $L = 0$  is the same. As shown in Fig. 6, the active impedance obtained using the MB-CBFM with  $L = 0$  converges to that of the infinite array as the size of the array increases. This implies that the current distribution of the elements in the central region of the array can be assumed to be uniform when the size of the array is

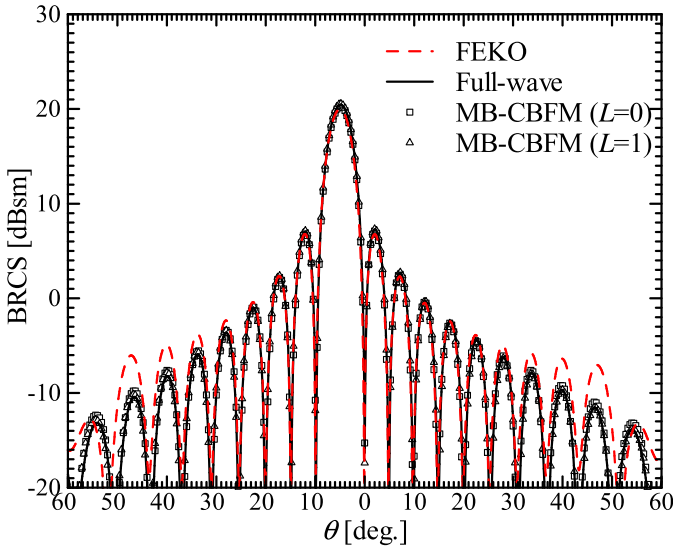


Fig. 7. BRCS of a  $25 \times 25$  microstrip dipole array scatterer [ $E_\theta$  on the  $yz$  plane,  $TM_z$  incidence,  $(\theta_i, \phi_i) = (5^\circ, 90^\circ)$ ].

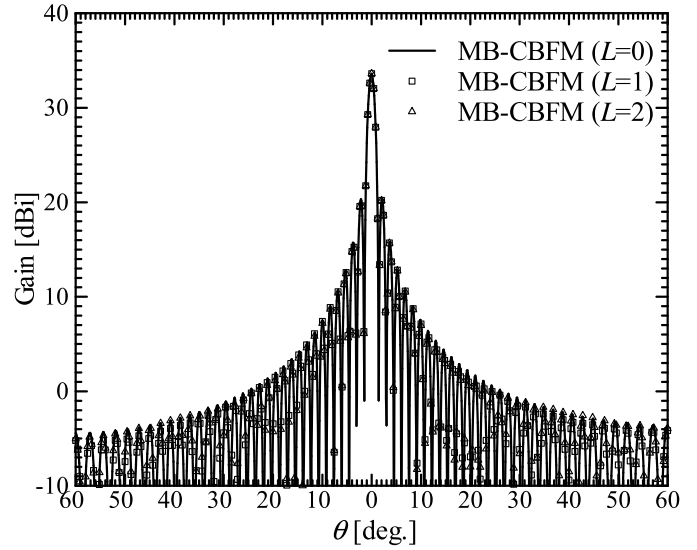


Fig. 9. Gain of a  $50 \times 50$  helical array antenna ( $E_\theta$  on the  $xz$  plane, in-phase and uniform excitation).

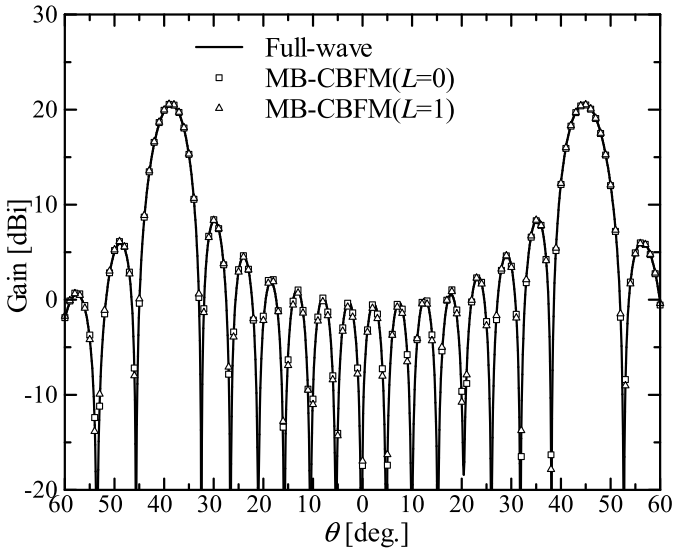


Fig. 8. Gain of a  $15 \times 15$  helical array antenna [ $E_\theta$  on the  $xz$  plane, mainlobe is directed to  $(\theta, \phi) = (45^\circ, 90^\circ)$ ].

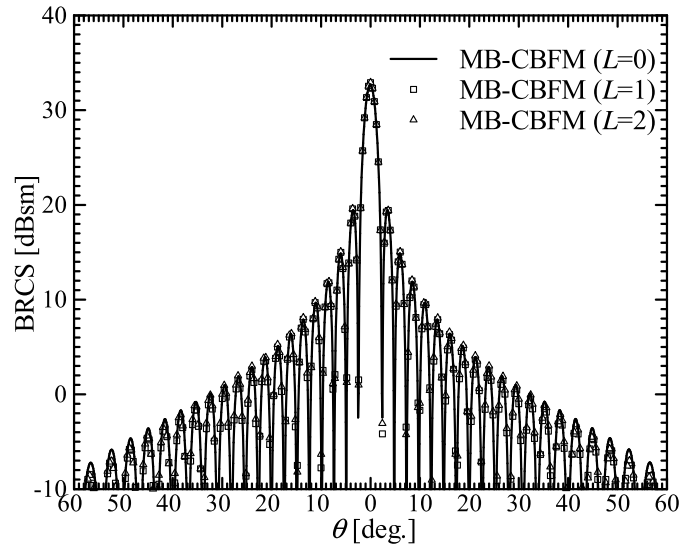


Fig. 10. BRCS of a  $50 \times 50$  microstrip dipole array scatterer [ $E_\theta$  on the  $yz$  plane,  $TM_z$  incidence,  $(\theta_i, \phi_i) = (0^\circ, 90^\circ)$ ].

large. According to these numerical results, it is concluded that the large-scale finite periodic array antenna can be analyzed using the MB-CBFM without neglecting the edge effect.

On the other hand, the width of macro blocks  $L$  in the edge region of the array seems to have relatively small impact on the accuracy of the bistatic radar cross section (BRCS) because the BRCS pattern is obtained from integration of current of the entire array, as seen in Fig. 7. The MB-CBFM results agree well with that obtained using full-wave analysis. Therefore, it can be concluded that the MB-CBFM works well to deal with a large-scale finite periodic array in a layered medium. The same phenomenon can be seen in the gain of the helical array antenna shown in Fig. 8. Therefore, it can be concluded that the width of macro blocks  $L$  in the edge region of the array should be considered in order to control the accuracy of

the near field (i.e., current distribution and active impedance) in the edge region of the array but has lesser effect on the accuracy of the far field (i.e., gain and BRCS) of the array. In order for the MB-CBFM to provide reliable results,  $L$  may be increased incrementally to gauge the convergence of the array fields of interest.

Large-scale finite periodic arrays which are difficult to solve exactly due to the limitation of computational cost may be solved quickly using the MB-CBFM. Numerical examples are a  $50 \times 50$  helical array antenna and the scattering from a  $50 \times 50$  microstrip dipole array. The total number of unknowns is  $N = 122\,500$  for the helical array antenna and  $N = 35\,000$  for the microstrip dipole array scatterer, respectively, each with  $M = 2500$  elements. The gain of the helical array antenna and BRCS of the microstrip dipole array scatterer

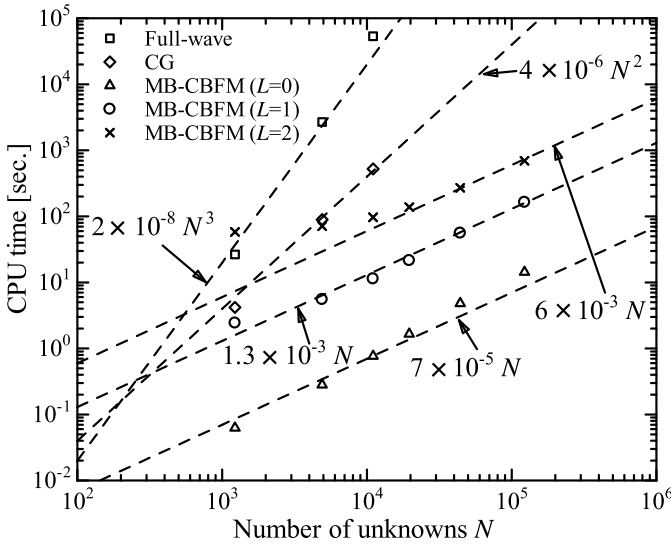


Fig. 11. CPU time (helical array).

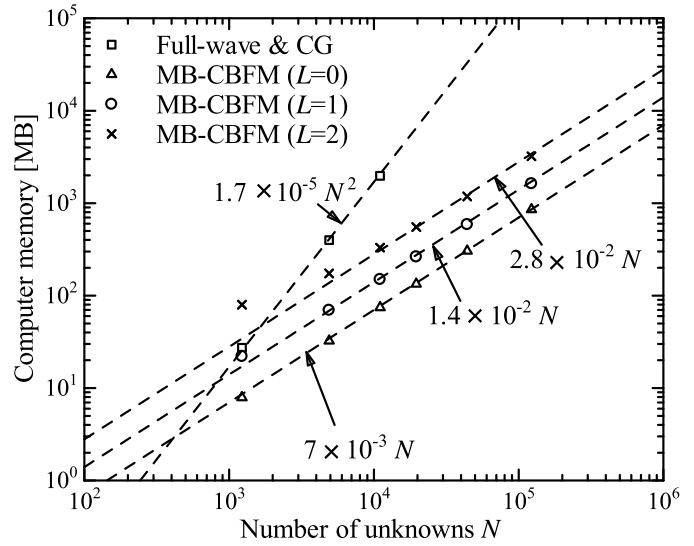


Fig. 13. Computer memory (helical array).

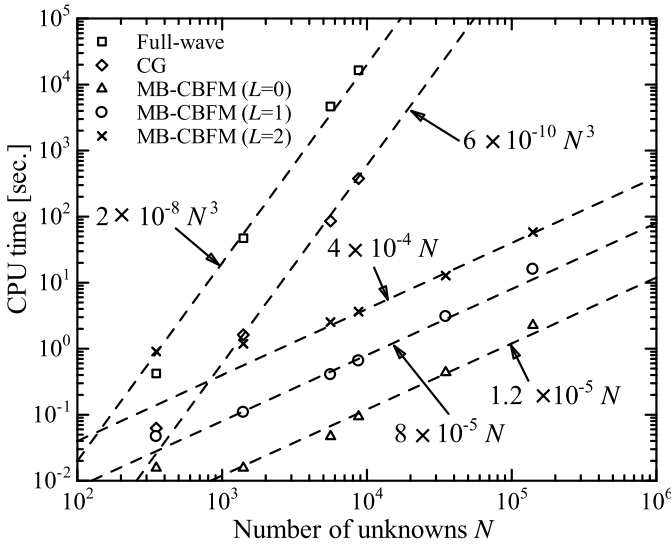


Fig. 12. CPU time (dipole array).

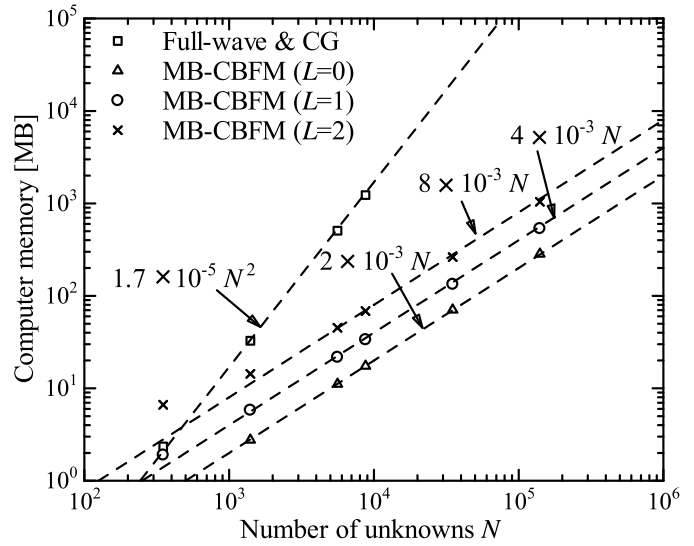


Fig. 14. Computer memory (dipole array).

are shown in Figs. 9 and 10, respectively. The CPU time except for impedance matrix filling and postprocessing is at most 695.9 s for the helical array antenna and 12.8 s for the microstrip dipole array scatterer, respectively. It is found that the large-scale finite arrays can be dealt with efficiently using the MB-CBFM.

The computational cost of the MB-CBFM is shown in Figs. 11–14. Here, the CPU time for impedance matrix filling and postprocessing is excluded in order to clearly show the main performance advantage of the MB-CBFM. The convergence criteria of the conjugate gradient method are the relative error set to  $10^{-4}$ . As shown in Figs. 11 and 12, the order of the CPU time of the CG method depends on the problem to be solved. Iterative solvers such as the CG method suffer from so-called ill-conditioned problems. For example, the order of the CPU time of the CG method is  $O(N^3)$  for the microstrip dipole array because the problem is ill-conditioned

and the number of iterations is proportional to  $N$ , while the helical array is  $O(N^2)$  because a relatively small number of iterations were needed. Therefore, it is difficult to predict the order of the CPU time of iterative solvers in advance. On the other hand, it is found that both CPU time and computer memory of the MB-CBFM are  $O(N)$  when the size of the array is large. The MB-CBFM is based on direct solvers so the order of its CPU time can be predicted analytically as shown in Table I. In addition, the periodicity of the array is fully utilized and the CBFs for macro blocks are obtained without extra computational cost. The resultant CPU time and computer memory of the MB-CBFM are quite small.

The CPU time for each process of the MB-CBFM is summarized in Table II. Here, the total CPU time including impedance matrix filling and postprocessing is also shown. It is found that the CPU time of the MB-CBFM in most cases is dominated by the calculation of the impedance matrix,

TABLE II  
CPU TIME OF THE MB-CBFM (s)

Analysis model	Helical array antenna ( $50 \times 50$ )			Microstrip dipole array antenna ( $50 \times 50$ )		
Width of the Edge regions $L$	$L = 0$	$L = 1$	$L = 2$	$L = 0$	$L = 1$	$L = 2$
Calculation of impedance matrix	333.6			4333.3		
Calculation of CBFs in blocks	0.02	0.9	26.5	0 (Negligibly small)	0.02	0.4
Calculation of $\mathbf{u}$ vectors	13.8	117.7	316.2	0.25	1.9	4.7
Calculation of reduced matrix	0.5	44.7	326.5	0.02	1	7.1
Inversion of reduced matrix	0.03	0.9	26.7	0.2	0.2	0.6
Postprocessing	140.1	148.9	156.1	283.4	284.7	283.5
Total	488	646.7	1185.6	4617.2	4621.1	4629.6

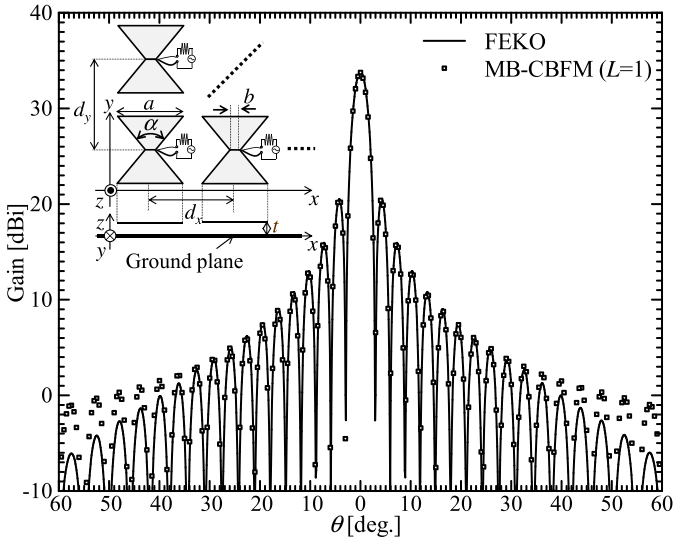


Fig. 15. Gain of a  $30 \times 30$  bowtie array antenna ( $E_\phi$  on the  $xz$  plane,  $f = 300$  MHz,  $a = \sqrt{2}/4$  m,  $b = 0.04$  m,  $\alpha = 70^\circ$ ,  $d_x = d_y = 0.65$  m,  $t = 0.25$  m,  $K = 64$ , uniform amplitude, and in-phase excitation).

especially for the dipole array due to the computation of the layered media Green's function. However, the cost is  $O(N)$  due to the Toeplitz structure of the array, and only needs to be done once for most array problems of interest as discussed earlier.

Finally, a bowtie array antenna was analyzed in order to demonstrate the performance of our MB-CBFM for arbitrary and practical antennas. Bowtie antenna elements are discretized into triangular elements using Rao–Wilton–Glisson basis function [36]. Fig. 15 shows the gain pattern of a  $30 \times 30$  bowtie array antenna. It is found that the gain pattern of the MB-CBFM agrees well with that of FEKO. The total number of unknowns is  $N = 57\,600$  and FEKO requires 103 921 s for LU decomposition while the MB-CBFM requires only 178 s. Therefore, the MB-CBFM is also efficient and accurate for the numerical analysis of arbitrary and practical array antennas.

#### IV. CONCLUSION

In this paper, a novel CBFM (MB-CBFM) for a large-scale finite periodic array has been proposed. The MB-CBFM utilizes blocks and macro blocks in order to reduce the computational cost greatly. According to array theory, the CBFs for the macro blocks are easily obtained from those of the blocks without extra computational cost. Numerical simulations have

demonstrated the accuracy, efficiency, and robustness of the MB-CBFM. The computational cost of the MB-CBFM described here is  $O(N)$ . In this paper, the MB-CBFM focuses on a large-scale periodic array excited by sources with uniform amplitude and linear phase. The MB-CBFM may be extended to more general nonuniform excitations in the future.

#### ACKNOWLEDGMENT

The authors would like to thank the staff at the Cyberscience Center, Tohoku University, for their helpful advice.

#### REFERENCES

- [1] Y. Konishi, "Phased array antennas," *IEICE Trans. Commun.*, vol. E86-B, no. 3, pp. 954–967, Mar. 2003.
- [2] M. Ando, "Planar waveguide arrays for millimeter wave systems," *IEICE Trans. Commun.*, vol. E93-B, no. 10, pp. 2504–2513, Oct. 2010.
- [3] M. Ohira, H. Deguchi, M. Tsuji, and H. Shigesawa, "Novel dual-resonant and dual-polarized frequency selective surface using eight-legged element and its experimental verification," *IEICE Trans. Electron.*, vol. E88-C, no. 12, pp. 2229–2235, Dec. 2005.
- [4] J. Huang and J. A. Encinar, *Reflectarray Antennas*. Hoboken, NJ, USA: Wiley, 2008.
- [5] L. Li *et al.*, "Novel broadband planar reflectarray with parasitic dipoles for wireless communication applications," *IEEE Antennas Wireless Propag. Lett.*, vol. 8, pp. 881–885, 2009.
- [6] L. Li *et al.*, "Frequency selective reflectarray using crossed-dipole elements with square loops for wireless communication applications," *IEEE Trans. Antennas Propag.*, vol. 59, no. 1, pp. 89–99, Jan. 2011.
- [7] J. F. Li, Q. Chen, Q. W. Yuan, and K. Sawaya, "Reflectarray element using interdigital gap loading structure," *Electron. Lett.*, vol. 47, no. 2, pp. 83–85, Jan. 2011.
- [8] R. F. Harrington, *Field Computation by Moment Methods*. New York, NY, USA: Macmillan, 1968.
- [9] B. A. Munk, *Frequency Selective Surfaces: Theory and Design*. Hoboken, NJ, USA: Wiley, 2000.
- [10] D. S. Janning and B. A. Munk, "Effects of surface waves on the currents of truncated periodic arrays," *IEEE Trans. Antennas Propag.*, vol. 50, no. 9, pp. 1254–1265, Sep. 2002.
- [11] J. M. Song and W. C. Chew, "Multilevel fast-multipole algorithm for solving combined field integral equations of electromagnetic scattering," *Microw. Opt. Technol. Lett.*, vol. 10, no. 1, pp. 14–19, Sep. 1995.
- [12] J. Song, C.-C. Lu, and W. C. Chew, "Multilevel fast multipole algorithm for electromagnetic scattering by large complex objects," *IEEE Trans. Antennas Propag.*, vol. 45, no. 10, pp. 1488–1493, Oct. 1997.
- [13] E. Bleszynski, M. Bleszynski, and T. Jaroszewicz, "AIM: Adaptive integral method for solving large-scale electromagnetic scattering and radiation problems," *Radio Sci.*, vol. 31, no. 5, pp. 1225–1251, 1996.
- [14] T. K. Sarkar, E. Arvas, and S. M. Rao, "Application of FFT and the conjugate gradient method for the solution of electromagnetic radiation from electrically large and small conducting bodies," *IEEE Trans. Antennas Propag.*, vol. AP-34, no. 5, pp. 635–640, May 1986.
- [15] H. Zhai, Q. Chen, Q. Yuan, K. Sawaya, and C. Liang, "Analysis of large-scale periodic array antennas by CG-FFT combined with equivalent sub-array preconditioner," *IEICE Trans. Commun.*, vol. E89-B, no. 3, pp. 922–928, Mar. 2006.

- [16] H. Zhai, Q. Yuan, Q. Chen, and K. Sawaya, "Preconditioners for CG-FMM-FFT implementation in EM analysis of large-scale periodic array antennas," *IEICE Trans. Commun.*, vol. E90-B, no. 3, pp. 707–710, Mar. 2007.
- [17] J. Heinstadt, "New approximation technique for current distribution in microstrip array antennas," *Electron. Lett.*, vol. 29, no. 21, pp. 1809–1810, Oct. 1993.
- [18] S. Ooms and D. De Zutter, "A new iterative diakoptics-based multilevel moments method for planar circuits," *IEEE Trans. Microw. Theory Techn.*, vol. 46, no. 3, pp. 280–291, Mar. 1998.
- [19] E. Suter and J. R. Mosig, "A subdomain multilevel approach for the efficient MoM analysis of large planar antennas," *Microw. Opt. Technol. Lett.*, vol. 26, no. 4, pp. 270–277, Aug. 2000.
- [20] L. Matekovits, V. A. Laza, and G. Vecchi, "Analysis of large complex structures with the synthetic-functions approach," *IEEE Trans. Antennas Propag.*, vol. 55, no. 9, pp. 2509–2521, Sep. 2007.
- [21] W. B. Lu, T. J. Cui, Z. G. Qian, X. X. Yin, and W. Hong, "Accurate analysis of large-scale periodic structures using an efficient sub-entire-domain basis function method," *IEEE Trans. Antennas Propag.*, vol. 52, no. 11, pp. 3078–3085, Nov. 2004.
- [22] P. Du, B.-Z. Wang, and H. Li, "An extended sub-entire domain basis function method for finite periodic structures," *IEEE Antennas Wireless Propag. Lett.*, vol. 7, pp. 404–407, 2008.
- [23] V. V. S. Prakash and R. Mittra, "Characteristic basis function method: A new technique for efficient solution of method of moments matrix equations," *Microw. Opt. Technol. Lett.*, vol. 36, no. 2, pp. 95–100, Jan. 2003.
- [24] W. B. Lu, T. J. Cui, X. X. Yin, Z. G. Qian, and W. Hong, "Fast algorithms for large-scale periodic structures using subentire domain basis functions," *IEEE Trans. Antennas Propag.*, vol. 52, no. 11, pp. 3078–3085, Nov. 2004.
- [25] W. B. Lu, T. J. Cui, and H. Zhao, "Acceleration of fast multipole method for large-scale periodic structures with finite sizes using sub-entire-domain basis functions," *IEEE Trans. Antennas Propag.*, vol. 55, no. 2, pp. 414–421, Feb. 2007.
- [26] L. Hu, L.-W. Li, and R. Mittra, "Electromagnetic scattering by finite periodic arrays using the characteristic basis function and adaptive integral methods," *IEEE Trans. Antennas Propag.*, vol. 58, no. 9, pp. 3086–3090, Sep. 2010.
- [27] J. Hu, W. Lu, H. Shao, and Z. Nie, "Electromagnetic analysis of large scale periodic arrays using a two-level CBFs method accelerated with FMM-FFT," *IEEE Trans. Antennas Propag.*, vol. 60, no. 12, pp. 5709–5716, Dec. 2012.
- [28] K. Konno, R. J. Burkholder, and Q. Chen, "Fast numerical analysis of finite periodic dipole array antenna embedded in thin-stratified medium using novel characteristic basis function method," in *Proc. IEICE Gen. Conf.*, Mar. 2016, pp. 1–2.
- [29] K. Konno, Q. Chen, and R. J. Burkholder, "Numerical analysis of finite periodic array antenna using novel characteristic basis function method," in *Proc. IEEE Int. Symp. Antennas Propag.*, Jun./Jul. 2016, pp. 49–50.
- [30] K. Konno, Q. Chen, K. Sawaya, and T. Sezai, "Optimization of block size for CBFM in MoM," *IEEE Trans. Antennas Propag.*, vol. 60, no. 10, pp. 4719–4724, Oct. 2012.
- [31] J. H. Richmond and N. Geary, "Mutual impedance of nonplanar-skew sinusoidal dipoles," *IEEE Trans. Antennas Propag.*, vol. AP-23, no. 3, pp. 412–414, May 1975.
- [32] W. C. Chew, J. L. Xiong, and M. A. Saville, "A matrix-friendly formulation of layered medium Green's function," *IEEE Antennas Wireless Propag. Lett.*, vol. 5, no. 1, pp. 490–494, Dec. 2006.
- [33] Y. P. Chen, W. C. Chew, and L. Jiang, "A new Green's function formulation for modeling homogeneous objects in layered medium," *IEEE Trans. Antennas Propag.*, vol. 60, no. 10, pp. 4766–4776, Oct. 2012.
- [34] A. Köksal and J. F. Kauffman, "Mutual impedance of parallel and perpendicular coplanar surface monopoles," *IEEE Trans. Antennas Propag.*, vol. 39, no. 8, pp. 1251–1256, Aug. 1991.
- [35] K. Konno, Q. Chen, and R. J. Burkholder, "Fast computation of layered media Green's function via recursive Taylor expansion," *IEEE Antennas Wireless Propag. Lett.*, vol. 16, pp. 1048–1051, 2017.
- [36] S. M. Rao, D. R. Wilton, and A. W. Glisson, "Electromagnetic scattering by surfaces of arbitrary shape," *IEEE Trans. Antennas Propag.*, vol. AP-30, no. 3, pp. 409–418, May 1982.



**Keisuke Konno** (M'12) received the B.E., M.E., and D.E. degrees from Tohoku University, Sendai, Japan, in 2007, 2009, and 2012, respectively.

He was a Visiting Scholar with the Electroscience Laboratory, The Ohio State University, Columbus, OH, USA, from 2015 to 2017. Since 2012, he has been with the Department of Communications Engineering, Graduate School of Engineering, Tohoku University, where he is currently an Assistant Professor. His current research interests include computational electromagnetics, array antennas, and

reflectarrays.

Dr. Konno is a member of IEICE. He received the JSPS Post-Doctoral Fellowships for Research Abroad. He was a recipient of the Encouragement Award for Young Researcher and Most Frequent Presentations Award in 2010 from the Technical Committee on Antennas and Propagation of Japan, the Young Researchers Award in 2011 from the Institute of Electronics, Information and Communication Engineers of Japan, the IEEE EMC Society Sendai Chapter Student Brush-up Session and EMC Sendai Seminar Student Best Presentation Award in 2011, and the JSPS Washington Director Award in 2016.



**Qiang Chen** (M'94–SM'12) received the B.E. degree from Xidian University, Xi'an, China, in 1986, and the M.E. and D.E. degrees from Tohoku University, Sendai, Japan, in 1991 and 1994, respectively.

He is currently a Chair Professor with the Electromagnetic Engineering Laboratory, Department of Communications Engineering, Faculty of Engineering, Tohoku University. His current research interests include antennas, microwave and millimeter wave, electromagnetic measurement, and computational

electromagnetics.

Dr. Chen is a member of the IEICE. He was a recipient of the Young Scientists Award in 1993 and the Best Paper Award and Zen-ichi Kiyasu Award in 2009 from the Institute of Electronics, Information and Communication Engineers (IEICE). He served as the Chair of the IEICE Technical Committee on Photonics-Applied Electromagnetic Measurement from 2012 to 2014 and the Vice Chair of the IEEE Antennas and Propagation Society Japan Chapter from 2012 to 2013. He is the Chair of the IEICE Technical Committee on Wireless Power Transfer. He was the Secretary and Treasurer of the IEEE Antennas and Propagation Society Tokyo Chapter in 1998, the Secretary of the Technical Committee on Electromagnetic Compatibility of IEICE from 2004 to 2006, the Secretary of the Technical Committee on Antennas and Propagation of IEICE from 2008 to 2010, and an Associate Editor of the *IEICE Transactions on Communications* from 2007 to 2012.



**Robert J. Burkholder** (S'85–M'89–SM'97–F'05) received the B.S., M.S., and Ph.D. degrees in electrical engineering from The Ohio State University, Columbus, OH, USA, in 1984, 1985, and 1989, respectively.

Since 1989, he has been with the Electroscience Laboratory, Department of Electrical and Computer Engineering, The Ohio State University, where he is currently a Research Professor and an Interim Director. He has contributed extensively to the electromagnetic scattering analysis of large and complex geometries, and targets in the presence of rough surfaces and microwave imaging through urban structures. His current research interests include high-frequency asymptotic techniques and their hybrid combination with numerical techniques for solving large-scale electromagnetic radiation, propagation, and scattering problems.

Dr. Burkholder is an elected Full Member of the International Union of Radio Scientists and Commission B and a member of the Applied Computational Electromagnetics Society. He is currently serving as a Track Editor of the IEEE TRANSACTIONS ON ANTENNAS AND PROPAGATION.